



1 **Mist Cannon Trucks Can Exacerbate Secondary**
2 **Organic Aerosol Formation and PM_{2.5} Pollution**
3 **in the Road Environment**

4

5 Yu Xu¹, Xin-Ni Dong², Chen He³, Dai-She Wu⁴, Hong-Wei Xiao¹, Hua-Yun Xiao^{1,*}

6

7 ¹School of Environmental Science and Engineering, Shanghai Jiao Tong University,
8 Shanghai 200240, China

9 ²Jiangxi Province Science and Technology Information Institute, Nanchang 330000,
10 China

11 ³State Key Laboratory of Heavy Oil Processing, China University of Petroleum, Beijing
12 102249, China

13 ⁴School of Resource, Environmental and Chemical Engineering, Nanchang University,
14 Nanchang 330031, China

15

16

17

18 *Corresponding author: Hua-Yun Xiao

19 E-mail: xiaohuayun@sjtu.edu.cn

20

Phone: +86-173-0183-7060

21

22

23

24



25 **Abstract:** Mist cannon trucks have been widely applied in megacities in China to
26 reduce the road dust. Their practical effect on controlling the formation of secondary
27 organic aerosol and fine particles remains unknown. We characterized the chemical
28 composition variations in $PM_{2.5}$ collected on the road sides with the simulated
29 operations of mist cannon truck and traditional sprinkling truck via Fourier transform
30 ion cyclotron resonance mass spectrometry and ion chromatography. The mass
31 concentrations of water-soluble organic carbon in $PM_{2.5}$ showed a significant increase
32 (62-70%) after air spraying. Further, we found that secondary organic aerosols,
33 particularly organic nitrates, increased significantly via the interactions of reactive gas-
34 phase organics, atmospheric oxidants, and aerosol liquid water after air spraying,
35 although the air spraying had a better effect on suppressing road dust than the ground
36 aspersion. Moreover, the formation of $PM_{2.5}$ in the road segment where the mist cannon
37 truck passed was promoted, with an increase of up to 13% in mass concentration after
38 25–35 minutes, on average. The application of mist cannon trucks undoubtedly worsens
39 the road atmospheric environment and causes health hazards to walking residents. The
40 overall results provide not only valuable insights to the formation processes of
41 secondary organic aerosols associated with aerosol liquid water in the road environment
42 but also management strategies to regulate the mist cannon truck operation in China.

43

44 **Keywords:** Mist cannon truck; Water mist; Secondary organic aerosols; $PM_{2.5}$; Process
45 and mechanism

46



47 **1 Introduction**

48 Over the past decade, the demand for effective road dust control has grown
49 dramatically due to the upgraded environmental protection policies and quality of life.
50 Traditionally, the sprinkling trucks with the ground aspersion work well for vehicle-
51 generated road dust. The newly developed mist cannon trucks are able to spray water
52 mist up to 120 meters away and 100 m high, with a droplet diameter of as small as 5
53 μm . They are considered to be more water-saving and efficient than the traditional
54 sprinkling truck (the ground aspersion). Thus, the mist cannon trucks have been widely
55 utilized by the local environmental bureau in recent years to achieve the target of strict
56 emission control in megacities in China (Wang et al., 2022). Traffic-related emissions
57 contribute a huge amount of volatile organic compounds (VOCs), nitrogen oxides
58 (NO_x), ammonia (NH_3), and fine aerosol particles ($\text{PM}_{2.5}$) to the urban atmosphere,
59 which exerts adverse impacts on human health and climate change (Deng et al., 2020;
60 Yang et al., 2022). However, no study has investigated whether and how the water mist
61 sprayed by mist cannon truck affects the road atmospheric environment in coordination
62 with traffic emissions.

63 As we know, the mist cannon trucks can spray a large amount of fine water mist in
64 a short time. It is expected that the air humidity of local road environment where the
65 mist cannon truck passed will increase sharply. Aerosol liquid water (ALW) exists in
66 the condensed phase as a function of particle chemical composition, particle
67 concentration, temperature (T), and relative humidity (RH) (Nguyen et al., 2015; Xu et
68 al., 2020a). Typically, an increase in RH can promote the rise in ALW concentration



69 (Guo et al., 2015). ALW, as a ubiquitous and abundant medium, can not only facilitate
70 partitioning of gas-phase water-soluble organics to the condensed phase but also drive
71 the formation of secondary organic aerosol (SOA) (Carlton and Turpin, 2013; Sareen
72 et al., 2017). The severe haze episodes in Beijing can even be partly attributed to the
73 interactions between ALW (or high RH) and aerosol organic components (Li et al., 2019;
74 Wang et al., 2021). In particular, 40–80% of fossil-fuel-derived primary organic
75 aerosols were found to be water-soluble (Qiu et al., 2019). Undoubtedly, there are large
76 knowledge gaps in our current understanding on ALW-related water-soluble SOA
77 formation in the road environment with mist cannon truck operation.

78 Although few studies have systematically evaluated the ability of mist cannon
79 truck to remove road dust, it is easy to understand that the tiny water droplets generated
80 by mist cannon system can indeed capture coarse particles (i.e., dropping dust to the
81 ground) more effectively than the water column sprayed by the traditional sprinkling
82 truck. However, fine particles (e.g., $PM_{2.5}$) are a major threat to urban atmospheric
83 environment and human health (Yue et al., 2020). Thus, it is necessary to understand
84 the removal effect of mist cannon truck on fine particles in road environment. Assessing
85 the impact of the mist cannon truck operation on road $PM_{2.5}$ pollution is also of great
86 significance for guiding future environmental protection initiatives.

87 In this study, we simulated the operation scenes of mist cannon truck and
88 traditional sprinkling truck on the sides of the urban road (Nanchang, eastern China)
89 and collected ambient $PM_{2.5}$ samples in these scenes. The molecular compositions of
90 water-soluble organic matter (WSOM) in $PM_{2.5}$ samples were resolved using ultrahigh-



91 resolution Fourier transform ion cyclotron resonance mass spectrometry (FT-ICR MS).
92 We also present the measurements of the relevant chemical parameters in PM_{2.5} samples
93 and the predicted ALW concentration. Furthermore, the variations of PM_{2.5}
94 concentrations in the road segment where the mist cannon truck passed were monitored.
95 The obtained results will clarify the impact of spraying water mist by mist cannon truck
96 on SOA formation and PM_{2.5} pollution control in the urban road environment for the
97 first time.

98

99 **2 Experimental Section**

100 **2.1 Study Site and Sample Collection.**

101 A branch road (provincial capital north 2nd road) that was selected as study area
102 was located in the centre of Nanchang (Eastern China) (**Figure S1a**). This area is
103 characterized by heavy traffic and high population density. There are no typical
104 pollution sources, such as factories and garbage treatment plants, within 30 km of the
105 study area. The trees on both sides of the road are very high and luxuriant (**Figure S1a**),
106 likely indicating that the atmosphere in this road environment is rarely disturbed by
107 strong winds and is relatively stable. The dominant species of the trees at the area is
108 camphor trees (*Cinnamomum Camphora*). Thus, the region is expected to be influenced
109 by both anthropogenic (vehicle exhausts) and biogenic VOCs.

110 Two sampling points with a distance of approximately 70 m were selected, which
111 were respectively on the roadside effected by air spray and ground aspersion (**Figure**
112 **S1b-e**). The air spraying 8 m above the ground was to simulate the water mist sprayed
113 by the mist cannon truck. In contrast, the ground aspersion with a height of 0.4 m above



114 the ground was designed to simulate the operation of traditional sprinkling truck.
115 Typically, thousands of oral fluid droplets emitted by loud speech will disappear in the
116 time range of 8 to 14 minutes in the stagnant air environment (Stadnytskyi et al., 2020).
117 It implied that the residence time of the fine water mist sprayed by the mist cannon
118 truck in the air may be longer than 8 min. As mentioned above, the luxuriant trees on
119 both sides of the road cause the atmosphere in the road environment to be relatively
120 stable with less disturbance by strong winds. Thus, the frequency of spraying water was
121 set to 1 minute spraying every 8 minutes (lower limit) in this study. The spraying was
122 controlled by an intelligent timing irrigation equipment (Nadster, China). It should be
123 noted that the diameter of the pores in the nozzle for air spraying is less than 0.8 mm,
124 while that in the nozzle for ground aspersion is approximately 6 mm.

125 Fine aerosol particles ($PM_{2.5}$) were collected onto the prebaked (500°C for ~10
126 hours) quartz fiber filters (Pallflex, Pall Corporation, USA) using a high-volume air
127 sampler (Series 2031, Laoying, China). Sampling at the above-mentioned two sites was
128 simultaneously performed from 23 March to 26 March, 2021. The duration of each
129 aerosol sampling was approximately 4 h (9:00–13:00 LT) every day. We observed that
130 the traffic flow on March 25 was higher than that on other days. The weather of
131 sampling periods was cloudy to sunny, sunny, sunny, and shower (only one short
132 precipitation event in the sampling period), corresponding an ambient average
133 temperature (T) of approximately 21 °C. The ambient average relative humidity (RH)
134 in those periods (23–25 March) ranged between 50% and 60%. The average RH can
135 reach 84–87% after air spraying. The ambient average RH was as high as 80% during



136 the period of 9:00–13:00 on 26 March. Thus, the water spraying operation was stopped
137 when the samples were collected on 26 March. The samples were stored at $-28\text{ }^{\circ}\text{C}$ prior
138 to the analysis. In addition, the mass concentrations of $\text{PM}_{2.5}$ were measured online
139 (Thermo Scientific 5030i, USA) from July to August 2021 near the trunk road where
140 the mist cannon truck frequently operated (**Figure S1a**). Specifically, $\text{PM}_{2.5}$
141 concentrations near road (81 road, Nanchang) were recorded at 5-minute intervals from
142 10 minutes before to 50 minutes after the mist cannon truck passed by.

143

144 2.2 Chemical Analysis.

145 A portion of each filter sample was ultrasonically extracted with Milli-Q water
146 (MQW, $18.2\text{ M}\Omega\text{ cm}$). WSOM in the extracting solution was further extracted using the
147 typical solid phase extraction (SPE) method, as indicated by previous studies (Dittmar
148 et al., 2008; Qiao et al., 2020; Xie et al., 2020). Briefly, the cartridge (PPL, 0.5 g, Agilent)
149 was rinsed with 18 mL of methanol (LC-MS grade, Thermo Fisher) and 18 mL of HCl
150 solution ($\text{pH} = 2$) in turn. Subsequently, the extracts with acidity adjusting ($\text{pH} = 2$)
151 were injected into cartridge. Acidified MQW (18 mL) and normal MQW (6 mL) were
152 added in turn to remove the salt and chloride ion trapped in the cartridge. After dryness
153 under a stream of N_2 , trapped OM was eluted using 15 mL of methanol. The eluted
154 solution was concentrated to 4 mL and then preserved at $-28\text{ }^{\circ}\text{C}$ until analysis. The
155 molecular compositions of WSOM in $\text{PM}_{2.5}$ samples were determined using a Bruker
156 Apex Ultra Fourier transform ion cyclotron resonance mass spectrometry (FT-ICR MS)
157 (Bruker, Germany) coupled to an Apollo II Electrospray ionization (ESI) (He et al.,



158 2020). The samples were injected into the ionization sources at a speed of $250 \mu\text{L h}^{-1}$.
159 The instrument was operated in the negative-ion mode, with a spray shield voltage of
160 4.0 kV. The mass range was set to m/z 200–800. One hundred and twenty-eight
161 continuous scans were acquired on each analysis to heighten the signal-to-noise ratio
162 of the mass spectrum. Detailed methodologies and data quality control during the
163 analysis were illustrated elsewhere (He et al., 2019; He et al., 2020).

164 Another filter cut was ultrasonically extracted with Milli-Q water for the
165 determination of water-soluble organic carbon (WSOC), water soluble total nitrogen
166 (WSTN), and inorganic ions. The mass concentrations of WSOC and WSTN in samples
167 were measured with a total organic carbon/total nitrogen analyser (Elementar vario,
168 Germany) (Xu et al., 2019). The mass concentration of WSOC was estimated to that of
169 WSOM using a conversion factor of 1.8 (Finessi et al., 2012; Müller et al., 2017; Simon
170 et al., 2011; Yttri et al., 2007). The mass concentrations of water-soluble inorganic ions,
171 such as SO_4^{2-} , NO_3^- , NH_4^+ , and K^+ , were measured using an ion chromatography
172 system (Dionex, Thermo, USA) (Xu et al., 2022; Xu et al., 2020b). The mass
173 concentration of water-soluble organic nitrogen (WSON) was calculated as the
174 difference in the concentrations between WSTN and inorganic nitrogen (i.e., $\text{NO}_3^- \text{N}$
175 + $\text{NO}_2^- \text{N}$ + $\text{NH}_4^+ \text{N}$) (Xu et al., 2020a). Ambient temperature and relative humidity
176 were measured using a temperature and humidity monitor (CEM 9880M, China).

177

178 **2.3 Data Processing and Statistical Analyses.**

179 The molecular formulas assigned from FT-ICR MS were classified into four main



180 compound groups in this study. These identified groups include CHO (containing only
181 C, H, and O), CHON (containing C, H, O, and N), CHOS (containing C, H, O, and S),
182 and CHONS (containing C, H, N, O, and S) (Song et al., 2018). The double-bond
183 equivalent (DBE) was calculated to describe the unsaturation degree of organic
184 compounds (**Supplementary Information**) (Qiao et al., 2020; Schmidt et al., 2017).
185 The modified aromaticity index (AI_{mod}) was also calculated to reflect the aromaticity of
186 organic molecules (**Supplementary Information**) (Koch and Dittmar, 2006; Schmidt
187 et al., 2017). The carbon oxidation state (OSc) can be used to indicate the evolving
188 composition of aerosol organics that underwent oxidation processes (Kroll et al., 2011).
189 The calculation of OSc was detailed in the **Supplementary Information**. According to
190 the oxygen-to-carbon (O/C) and hydrogen-to-carbon (H/C) elemental ratios, the
191 identified molecular formulas were further classified into five compound categories,
192 including unsaturated aliphatic-like, highly unsaturated-like, highly aromatic-like,
193 polycyclic aromatic-like, and saturated-like molecules (Sihui et al., 2021). These
194 classified compound categories were visualized in the van Krevelen diagram
195 (**Supplementary Information**).

196 The thermodynamic model ISORROPIA-II was applied to calculate the mass
197 concentrations of ALW driven by inorganic components (Guo et al., 2015; Tan et al.,
198 2017; Xu et al., 2022). The model predicts the inorganic ALW based on particle mass
199 concentrations of inorganic species, RH, and ambient T (**Supplementary Information**).
200 Particle hygroscopicity is also influenced by organics in aerosol particles (Cruz and
201 Pandis, 2000; Sareen et al., 2013). The impact of organic faction on aerosol water is



202 complex and depends on the composition of organic matter (Nguyen et al., 2016). In
203 this study, the mass concentration of water associated with aerosol organic fraction was
204 predicted according to a previously reported model with the
205 Zdanovskii–Stokes–Robinson mixing rule (**Supplementary Information**) (Nguyen et
206 al., 2015; Nguyen et al., 2016).

207

208 **3 Results and Discussion**

209 **3.1 Chemical Characteristics of PM_{2.5} in Different Road Segments.**

210 **Figure 1** compares the differences in the chemical composition of PM_{2.5} collected
211 in the air spray road segment and ground aspersion road segment. WSOM was the
212 dominant component irrespective of the weather and road section where the samples
213 were collected, which accounted for 30–40% of the water-soluble aerosols (**Figure1a–**
214 **c**). From March 23 to March 25, the mass concentrations and fractions of WSOM
215 (/WSOC) were higher in the air spray road segment than in the ground aspersion road
216 segment. For the case without water spray treatment (as reference group), the chemical
217 composition characteristics of PM_{2.5} samples collected from those two adjacent road
218 segments only showed small differences (**Figure1d,h,i**). Obviously, these variations in
219 the mass concentrations and fractions of WSOM can be attributed to the difference in
220 water-soluble SOA yield or formation pathway caused by different water spray
221 treatments.

222 The variation pattern of ALW was similar to that of WSOC during the study
223 periods (**Figure1e–h**). Moreover, the mass concentrations of WSON also tended to



224 decrease from the air spray road segment to the ground aspersion road segment. Linear
225 regression analysis for all data showed that the mass concentrations of ALW were
226 significantly positively ($P < 0.01$) correlated with those of WSOC and WSON, with R^2
227 of 0.84 and 0.75, respectively. The results were consistent with those obtained by the
228 previous studies conducted in an agriculture area in Italy (Hodas et al., 2014) and a
229 suburban forest site in Tokyo (Xu et al., 2020a). Those studies suggested that the ALW
230 dependence of reactive gas uptake and subsequent aqueous reactions significantly
231 contributed the production of WSOC and WSON. Thus, the increase in ALW
232 concentration after air spraying can promote the formation of aqueous SOA in the road
233 environment.

234 Nitrate and sulfate were the most abundant inorganic components (**Figure 1a–d**),
235 which have been identified as typical factors controlling ALW (Hodas et al., 2014).
236 From the air spray road segment to the ground aspersion road segment, the decrease in
237 nitrate concentration was more significant than that in sulfate concentration (**Figure 1e–**
238 **f**). Moreover, the concentration of nitrate significantly correlated with that of ALW (P
239 < 0.01 , $R^2 = 0.7$). In contrast, the sulfate did not show a strong correlation with ALW
240 ($R^2 = 0.3$). In the region with large NO_x and ammonia emissions (traffic-related) (Yang
241 et al., 2022), the formation of nitrate could be promoted by enhanced RH (24–43% of
242 increase) caused by air spraying. This is partly consistent with the thermodynamics of
243 ammonium nitrate formation (Hodas et al., 2014; Mozurkewich, 1993). Thus, the
244 increase in ALW concentration after air spraying was mainly driven by RH and locally
245 (traffic emissions) formed nitrate aerosol. It also implied that the formation of nitrate



246 and ALW is mutually reinforcing (Chen et al., 2022).

247 Interestingly, Ca^{2+} and Mg^{2+} showed a significant increase in the concentration
248 from the air spray road segment to the ground aspersion road segment (**Figure 1i–k**),
249 which was contrary to the case of other components (e.g., WSOC, ALW and nitrate). In
250 addition, during March 26 without water spray treatment, the differences in both Ca^{2+}
251 and Mg^{2+} concentrations between those two adjacent road segments were almost
252 negligible (**Figure 1f**). It is well known that Ca^{2+} and Mg^{2+} are typical crustal materials
253 and are mainly enriched in atmospheric coarse particles (Chen and Chen, 2008). Thus,
254 a decrease in Ca^{2+} and Mg^{2+} concentrations after air spraying implied that the water mist
255 sprayed by mist cannon truck had a better effect on suppressing road dust than the
256 ground aspersion by traditional sprinkling truck.

257

258 **3.2 General Molecular Characteristics of Water-Soluble Organic Aerosols.**

259 Thousands of molecular formulas (5966–8102) were observed in WSOM in $\text{PM}_{2.5}$
260 collected from road environment (**Table 1**). The CHO molecular formulas (1089–2037)
261 accounted for 20–25% in all molecular formulas. CHO compounds were classified by
262 the number of oxygen atoms in their molecules, according to which the subgroups
263 ranged from O_2 to O_{15} (**Figure 2**). The number and intensity of dominated O_5 – O_{10}
264 subgroups accounted for 72–85% and 71–86% of the total compounds, respectively;
265 moreover, these percentages were higher than the results reported for aerosols in Beijing
266 (Xie et al., 2020). The average H/C and O/C ratios of CHO compounds varied from
267 1.08 to 1.24 and from 0.42 to 0.49, respectively (**Table S1**). The average O/C ratios



268 were higher than the value (0.03 ± 0.11) obtained from typical urban aerosols (Beijing,
269 China), while the H/C ratios showed relatively small differences between our results
270 and observation results in Beijing (1.14 ± 0.37) (Xie et al., 2020). These dissimilarities
271 might be attributed to the more complex sources of urban aerosols compared to aerosols
272 collected from road environment.

273 The average H/C and O/C ratios of CHON compounds ranged from 1.05 to 1.21
274 and 0.42 to 0.51, respectively (**Table S1**). The H/C ratio ranges of CHON compounds
275 in this study overlapped with those measured in previous studies (Sihui et al., 2021; Xie
276 et al., 2020). However, the O/C ratios of CHON compounds were relatively higher in
277 road-derived aerosols than in aerosols or snow collected in urban areas (building roof)
278 (Sihui et al., 2021; Xie et al., 2020), which implied the importance of source strength
279 (e.g., vehicle emissions) to aerosol chemical composition. The number of CHON
280 formulas (1501–2685) was much higher than that of CHO formulas (**Table 1**). The
281 assigned CHON formulas were further divided into CHON_1 (N_1O_2 – N_1O_{16}), CHON_2
282 (N_2O_2 – N_2O_{13}), and CHON_3 (N_3O_2 – N_3O_{13}) groups (**Figure 2**). CHON_1 was found to be
283 the dominant nitrogen-containing species in all samples, which was consistent with
284 previous reports on urban aerosols and snow (Sihui et al., 2021; Xie et al., 2020).
285 Moreover, the CHON_1 compounds with $\text{O/N} > 2$ contributed 99.2% – 100.0% to total
286 CHON_1 species in all samples. The CHON_2 compounds with $\text{O/N} > 2$ accounted for
287 90.2–100.0% of CHON species containing two nitrogen atoms. For CHON_3 group, the
288 proportion of nitrogen-containing compounds with $\text{O/N} > 2$ was 53.0–61.8%. The
289 CHON species with $\text{O/N} > 2$, which allows an assignment of oxidized-form nitrogen,



290 are preferentially ionized in negative electrospray ionization mode (Lin et al., 2015;
291 Sihui et al., 2021). Studies on the compositions of organic matter in urban rainwater
292 and aerosols have suggested that numerous CHON compounds contained oxidized
293 nitrogen function groups (e.g., $-\text{ONO}_2$) and that NO_x -related oxidation processes are
294 responsible for the formation of these CHON compounds (Altieri et al., 2009; Lee et
295 al., 2016). Thus, the CHON compounds with $\text{O/N} > 2$ in our $\text{PM}_{2.5}$ samples can be
296 assumed to be substantially in an oxidized form (e.g., organic nitrates).

297 **Figure 2** also shows the differences in the number of CHO and CHON species
298 between the air spray road segment and ground aspersion road segment. The abundance
299 of each O_n subgroup in CHO compounds considerably enhanced after air spraying,
300 especially the subgroups of O_5 – O_{11} . In contrast, the number of CHO species for these
301 two cases without water spray treatment showed a considerably small difference
302 (**Figure 2d**). In general, the total number of CHO compounds increased significantly
303 after air spraying (**Table 1** and **Figure 2**). However, there was no significant change for
304 the total number of CHO species between the two cases without water spray treatment.
305 These findings implied that increased ALW via the air spraying can contribute
306 substantially to the formation of CHO compounds with a more oxygenated state.

307 The number of CHON compounds decreased significantly from the air spray road
308 segment to the ground aspersion road segment, a variation pattern of which was similar
309 to that of CHO compounds (**Figure 2** and **Table 1**). Furthermore, the decrease in
310 number from the air spray road segment to the ground aspersion road segment was more
311 remarkable for CHON_1 compounds than for CHON_2 compounds. In contrast, the



312 variation in the number of CHON_3 after air spraying was less significant than that of
313 CHON_{1-2} compounds. In addition, insignificant change in the number of CHON
314 compounds was found in $\text{PM}_{2.5}$ collected in the two road segments without water spray
315 (**Figure 2d**). As mentioned above, the potentially high abundance of organic nitrates
316 has been suggested in these road-derived aerosols. Thus, an increase in nitrogen-
317 containing compounds after air spraying indicated that the interactions among ALW,
318 traffic-derived reactive nitrogen and ambient VOCs play an important role in organic
319 nitrogen compound formation in aerosol fine particles. The current result can be partly
320 supported by that obtained by Xu et al. (2020a) in a suburban forest in Tokyo, Japan.
321 The authors suggested that ALW is a key driver for the formation of aerosol WSON
322 through secondary processes associated with atmospheric reactive nitrogen and
323 biogenic VOCs. For the sulfur-containing compounds, their molecular number just
324 showed a relatively small change after air spraying (**Figure S2**). It suggested that the
325 impact of ALW on sulfur-containing compound formation was weaker than that of ALW
326 on the formation of CHO and CHON compounds in this road environment.

327

328 **3.3 Newly Emerging CHO and CHON Species under the Influence of High ALW.**

329 The molecular compositions of CHO compounds in $\text{PM}_{2.5}$ in the van Krevelen
330 diagram were scattered across wider ranges in the air spray road segment than in the
331 ground aspersion road segment, particularly in the sunny days (24 and 25 March)
332 (**Figure 3**). The result may be attributed to the increasing molecular diversity caused by
333 ALW-related atmospheric processes. It also implied the importance of photochemical



334 reactions in CHO compound formation. Further, the unique CHO compounds were
335 identified between PM_{2.5} samples in the air spray road segment (/no water spray road
336 segment (A)) and the ground aspersion road segment (/no water spray road segment (B))
337 (**Figure S3**). On 23 March and 24 March, the newly emerging CHO compounds after
338 air spraying were dominated by unsaturated aliphatic-like and highly unsaturated-like
339 compounds. However, both unsaturated-like species (unsaturated aliphatic-like and
340 highly unsaturated-like) and aromatic-like species (highly aromatic-like and polycyclic
341 aromatic-like) contributed significantly to the newly emerging CHO compounds after
342 air spraying on 25 March when the ALW and traffic flow were higher than other days
343 (**Figure S3**). Obviously, the formation of those unique CHO compounds was tightly
344 associated with increased ALW.

345 **Figure 4** shows the OSc of identified unique CHO molecules. The OSc values of
346 these CHO molecules were higher than those of primary vehicle exhausts (−2.0 to −1.9)
347 (Aiken et al., 2008). The OSc values of the secondary organic aerosol formed via the
348 reactions of anthropogenic and biogenic VOCs (e.g., isoprene, monoterpene, toluene,
349 alkane, and alkene) and oxidants (e.g., O₃ and/or •OH) varied from −1.1 to +1.0 (Kroll
350 et al., 2011; Li et al., 2021), which was within the OSc value ranges of CHO molecules
351 measured in this study. In addition, hydrocarbon-like organic aerosol (HOA) likely
352 linked with primary fresh vehicle exhausts (Sun et al., 2016) only accounted for less
353 than 6% of total unique CHO compounds (**Figure 4**). As mentioned previously, there
354 are dense trees on both sides of the road. Thus, these newly emerging CHO compounds
355 can be largely attributed to secondary processes associated with oxidation of vehicle



356 exhausts and biogenic VOCs by O_3 and/or $\bullet OH$. In addition, we also observed an
357 oligomerization trend (e.g., methylglyoxal ($C_3H_4O_2$) to form oligomers ($C_{4-7}H_{6-10}O_5$)
358 in particle phase) for CHO compounds after air spraying, particularly on 25 March with
359 a high ALW and a large traffic flow (**Figure S4c**). The overall results implied that the
360 water mist sprayed by mist cannon trucks can indeed enhance the abundance and
361 diversity of CHO compounds in fine aerosol particles via promoting gas-to-particle
362 partitioning of gas-phase oxidation products of VOCs and subsequent aqueous-phase
363 reactions.

364 For the CHON compounds, their molecular compositions were scattered across an
365 increased ranges in the van Krevelen diagram after air spraying (**Figure S5**). Moreover,
366 these newly emerging CHON molecules after air spraying showed a high diversity, as
367 shown in **Figure S6**. The group of $CHON_1$ was the dominant nitrogen-containing
368 compound in the identified unique CHON compounds. On 23 March and 24 March, the
369 mainly unique CHON compounds emerged during air spraying were unsaturated
370 aliphatic-like and highly unsaturated-like nitrogen-containing species. The number of
371 highly aromatic-like and polycyclic aromatic-like compounds that newly emerged also
372 increased significantly following increased traffic flow and ALW (25 March). The
373 results suggested that increases in ALW after air spraying can facilitate the formation
374 of particle-phase nitrogen-containing compounds (Hallquist et al., 2009; Xu et al.,
375 2020a).

376 Organic nitrates have been supposed to be abundant in our $PM_{2.5}$ samples collected
377 from road environment. It is well documented that atmospheric organic nitrates are



378 primary, secondary, and tertiary byproducts of anthropogenic and biogenic VOCs with
379 O_3 ($\bullet OH$) under the influence of NO_x or nitrate radicals (Lee et al., 2016; Sihui et al.,
380 2021; Yeh and Ziemann, 2014). In addition, numerous organic nitrates are known as
381 semivolatile compounds, with a partition between the gas and particle phases when they
382 are oxidized or photolyzed (Bean and Hildebrandt Ruiz, 2016). Recently, an oxidation
383 and hydrolysis mechanism associated with the atmospheric organic nitrates formation
384 has been proposed to interpret the potential origins or precursors of CHON compounds
385 (Sihui et al., 2021). In this study, we found that 68–82% of newly emerging $CHON_1$
386 compounds after air spraying can be explained by oxidation (e.g., R_1OH)-product (e.g.,
387 R_1ONO_2) pair (**Figure 5a-c**). It indicated that these newly emerging $CHON_1$
388 compounds were largely derived from the oxidation of CHO species under existence of
389 NO_x . A similar pattern was also observed in the newly emerging $CHON_2$ compounds
390 (**Figure S7**). The number of unique $CHON_1$ and $CHON_2$ compounds in the two cases
391 without water spray treatment was much less than that in the cases with air spraying
392 and ground aspersion (**Figure 5** and **Figure S7**). However, a significant oligomerization
393 trend for CHON compounds after air spraying was not observed after air spraying
394 (**Figure S8**). It should be pointed out that vehicle exhausts and roadside vegetation are
395 important sources for VOCs and NO_x in this road environment. These results suggested
396 that increased ALW caused by air spraying can serve as an abundant medium for the
397 formation of organic nitrates via CHO compounds as potential precursors.

398

399 **3.4 Environmental Implication.**



400 Misting cannon sprayers are commonly applied in greening maintenance and
401 conventional agriculture for the distribution of fertilizers, pesticides, and herbicides. In
402 recent years, misting cannon trucks are developed and serve as an excellent option for
403 road dust control due to the production of tiny water droplets that can drop dust to the
404 ground. In particular, it is a high-performance system of spraying disinfection in the
405 road environment during the COVID-19 epidemic period. For the first time, we provide
406 a detailed characterization of chemical compositions in road-derived $PM_{2.5}$ under the
407 influence of air spraying. Recent study conducted in a rural site (China) has suggested
408 that gaseous water-soluble organic compounds mainly partitioned to the organic phase
409 under the condition of RH less than 80% (relatively low ALW) but to ALW under the
410 humid condition ($RH > 80\%$, as air spraying operation), highlighting the importance of
411 high ALW in SOA formation processes (Lv et al., 2022). Our results verified the
412 formation of numerous new CHO and CHON compounds by ALW-related promoting
413 effect (**Figure 6**). In particular, the mass concentrations of WSOC in $PM_{2.5}$ increased
414 by 62–70% after air spraying. Clearly, although the air spraying by mist cannon system
415 could exert a better effect on suppressing road dust than the ground aspersion, as
416 discussed previously, air pollution induced by increased SOA will be exacerbated in the
417 road environment.

418 To further reveal the influence of air spraying on $PM_{2.5}$ pollution on the roadside,
419 we investigated the time series of percentage variation in $PM_{2.5}$ mass concentrations
420 after mist cannon truck operation at a low-speed (< 30 km/h) (**Figure 7**). At 25–35
421 minutes after the mist cannon truck passed, the increase proportion of $PM_{2.5}$



422 concentration on the roadside gradually reached the maximum (~13%, on average).
423 Subsequently, the proportion of increase in PM_{2.5} concentration gradually decreased,
424 reaching ~6% at 50 min after the mist cannon truck was operated. It should be noted
425 that the width of the road segment (81 road, Nanchang, China) where PM_{2.5} was
426 monitored is very large (~43 m). Thus, on conventional urban roads, the water mist
427 sprayed by mist cannon truck should exert a greater promoting effect on the formation
428 of PM_{2.5}. The overall results suggested that mist cannon truck cannot effectively reduce
429 the PM_{2.5} level in the road environment, but lead to aggravation of PM_{2.5} pollution.

430 The chemical composition of fine aerosol particles in the urban road atmosphere
431 is highly complex, including a lot of harmful organic compounds (polycyclic aromatic
432 hydrocarbons and nitro-aromatics), as indicated by our measurements and previous
433 study (Tong et al., 2016). Emissions from vehicles and roadside greening vegetation are
434 important anthropogenic and biogenic sources of reactive gas-phase OC and key
435 precursors to form SOA in urban areas (Gentner et al., 2012; Tong et al., 2016; Xu et
436 al., 2020a). In particular, organic aerosol composition in the road environment can be
437 strongly impacted by vehicle emissions (e.g., VOCs and NO_x) (Tong et al., 2016).
438 Inhalation of the particles containing harmful organics can be responsible for a number
439 of adverse health effects (Künzli et al., 2000). However, the wide application of mist
440 cannon truck by local environmental protection department undoubtedly accelerates the
441 formation processes of SOA and PM_{2.5} associated with ALW, which will further worsen
442 the urban road environment and cause health hazards to walking residents. Thus, the
443 present study provides the crucial information for the decision makers to regulate the



444 current mist cannon truck operation in many cities in China.

445

446 **4 Conclusions**

447 We investigated the changes in chemical compositions of PM_{2.5} collected from the
448 road sides of the urban road (Nanchang, eastern China) with the simulated operations
449 of mist cannon truck and traditional sprinkling truck. Moreover, we also conducted
450 online measurement of PM_{2.5} concentration in the urban road segment where the mist
451 cannon truck passed by. The mass concentrations of WSOC in PM_{2.5} increased
452 significantly (62-70%) from the ground aspersion road segment to the air spray road
453 segment. Similarly, ALW, mainly driven by RH and locally formed nitrate aerosol, also
454 showed a significant increase after air spraying. Moreover, we found that the mass
455 concentration of ALW in PM_{2.5} was significantly ($P < 0.01$) correlated with that of
456 WSOC and WSON. Thus, the increase of ALW after air spraying can promote the
457 formation of particle-phase water-soluble organics in the road environment. In addition,
458 a decrease in Ca²⁺ and Mg²⁺ concentrations after air spraying suggested that the water
459 mist sprayed by mist cannon truck exerted a better effect on suppressing road dust than
460 the ground aspersion by traditional sprinkling truck.

461 A comparison in the number of CHO and CHON species between the air spray
462 road segment and ground aspersion road segment suggested that the increase of ALW
463 after air spraying can enhance the abundance and diversity of CHO and CHON
464 compounds in fine aerosol particles. The newly emerging CHO compounds after air
465 spraying can be largely attributed to secondary processes associated with oxidation of



466 vehicle exhausts and biogenic VOCs by oxidants and oligomerization. Organic nitrates
467 were considered to be the abundant nitrogen-containing compounds in the $PM_{2.5}$
468 samples. Furthermore, we found that the newly emerging organic nitrates were largely
469 derived from the oxidation of CHO species under existence of NO_x .

470 At 25–35 minutes after the mist cannon truck passed, $PM_{2.5}$ concentration on the
471 roadside increased by up to 13%, on average. The proportion of increase in $PM_{2.5}$
472 concentration gradually decreased to ~6% at 50 min after the mist cannon truck was
473 operated. The overall results suggested that although mist cannon truck could exert a
474 better effect on suppressing road dust than the traditional sprinkling truck, air pollution
475 induced by increased SOA and $PM_{2.5}$ level will be exacerbated in the urban road
476 environment. Our findings provide new insights into the formation processes of SOA
477 associated with the water mist sprayed by mist cannon truck in the road atmospheric
478 environment.

479

480 **Data Availability**

481 The data presented in this paper can be accessed at zenodo
482 (DOI:10.5281/zenodo.7113675).

483

484 **Supporting Information**

485 Additional 1 table and 8 figures and details about parameter calculation, compound
486 categorization, and ALW prediction.

487



488 **Author contributions**

489 Conceptualization: Yu Xu, Hua-Yun Xiao, Dai-She Wu

490 Methodology: Yu Xu, Xin-Ni Dong, Chen He

491 Investigation: Xin-Ni Dong, Hong-Wei Xiao

492 Writing—original draft: Yu Xu

493 Writing—review & editing: Yu Xu

494

495 **Competing interests**

496 The authors declare no competing financial interest.

497

498 **Acknowledgements**

499 This study was kindly supported by Shanghai “Science and Technology Innovation

500 Action Plan” Shanghai Sailing Program through grant 22YF1418700 (Y. Xu) and the

501 Natural (Youth) Science Foundation of Jiangxi, China through grant 20212BAB213039

502 (Y. Xu).

503

504 **References**

505 Aiken, A. C., DeCarlo, P. F., Kroll, J. H., Worsnop, D. R., Huffman, J. A., Docherty, K.

506 S., Ulbrich, I. M., Mohr, C., Kimmel, J. R., Sueper, D., Sun, Y., Zhang, Q.,

507 Trimborn, A., Northway, M., Ziemann, P. J., Canagaratna, M. R., Onasch, T. B.,

508 Alfarra, M. R., Prevot, A. S. H., Dommen, J., Duplissy, J., Metzger, A.,

509 Baltensperger, U., Jimenez, J. L.: O/C and OM/OC Ratios of Primary,



- 510 Secondary, and Ambient Organic Aerosols with High-Resolution Time-of-
511 Flight Aerosol Mass Spectrometry, *Environ. Sci. Technol.*, 42(12): 4478-4485,
512 2008.
- 513 Altieri, K. E., Turpin, B. J., Seitzinger, S. P.: Oligomers, organosulfates, and nitrooxy
514 organosulfates in rainwater identified by ultra-high resolution electrospray
515 ionization FT-ICR mass spectrometry, *Atmos. Chem. Phys.*, 9(7): 2533-2542,
516 2009.
- 517 Bean, J. K., Hildebrandt Ruiz, L.: Gas-particle partitioning and hydrolysis of organic
518 nitrates formed from the oxidation of α -pinene in environmental chamber
519 experiments, *Atmos. Chem. Phys.*, 16(4): 2175-2184, 2016.
- 520 Carlton, A., Turpin, B.: Particle partitioning potential of organic compounds is highest
521 in the Eastern US and driven by anthropogenic water, *Atmos. Chem. Phys.*,
522 13(20): 10203-10214, 2013.
- 523 Chen, H. Y., Chen, L. D.: Importance of anthropogenic inputs and continental-derived
524 dust for the distribution and flux of water-soluble nitrogen and phosphorus
525 species in aerosol within the atmosphere over the East China Sea, *J. Geophys.*
526 *Res.: Atmos.*, 113: D11. DOI: 10.1029/2007JD009491., 2008.
- 527 Chen, Y., Wang, Y., Nenes, A., Wild, O., Song, S., Hu, D., Liu, D., He, J., Hildebrandt
528 Ruiz, L., Apte, J. S., Gunthe, S. S., Liu, P.: Ammonium Chloride Associated
529 Aerosol Liquid Water Enhances Haze in Delhi, India, *Environ. Sci. Technol.*,
530 2022.
- 531 Cruz, C. N., Pandis, S. N.: Deliquescence and hygroscopic growth of mixed inorganic-



- 532 organic atmospheric aerosol, *Environ. Sci. Technol.*, 34(20): 4313-4319, 2000.
- 533 Deng, F., Lv, Z., Qi, L., Wang, X., Shi, M., Liu, H.: A big data approach to improving
534 the vehicle emission inventory in China, *Nat. Commun.*, 11(1): 2801, 2020.
- 535 Dittmar, T., Koch, B., Hertkorn, N., Kattner, G.: A simple and efficient method for the
536 solid-phase extraction of dissolved organic matter (SPE-DOM) from seawater,
537 *Limnol. Oceanogr.: Meth.*, 6(6): 230–235, 2008.
- 538 Finessi, E., Decesari, S., Paglione, M., Giulianelli, L., Carbone, C., Gilardoni, S., Fuzzi,
539 S., Saarikoski, S., Raatikainen, T., Hillamo, R.: Determination of the biogenic
540 secondary organic aerosol fraction in the boreal forest by NMR spectroscopy,
541 *Atmos. Chem. Phys.*, 12(2): 941-959, 2012.
- 542 Gentner, D. R., Isaacman, G., Worton, D. R., Chan, A. W. H., Dallmann, T. R., Davis,
543 L., Liu, S., Day, D. A., Russell, L. M., Wilson, K. R., Weber, R., Guha, A.,
544 Harley, R. A., Goldstein, A. H.: Elucidating secondary organic aerosol from
545 diesel and gasoline vehicles through detailed characterization of organic carbon
546 emissions, *P. Natl. Acad. Sci. U. S. A.*, 109(45): 18318-18323, 2012.
- 547 Guo, H. Y., Xu, L., Bougiatioti, A., Cerully, K. M., Capps, S. L., Hite Jr, J., Carlton, A.,
548 Lee, S. H., Bergin, M., Ng, N.: Fine-particle water and pH in the southeastern
549 United States, *Atmos. Chem. Phys.*, 15(9): 5211-5228, 2015.
- 550 Hallquist, M., Wenger, J. C., Baltensperger, U., Rudich, Y., Simpson, D., Claeys, M.,
551 Dommen, J., Donahue, N., George, C., Goldstein, A.: The formation, properties
552 and impact of secondary organic aerosol: current and emerging issues, *Atmos.*
553 *Chem. Phys.*, 9(14): 5155-5236, 2009.



- 554 He, C., Pan, Q., Li, P., Xie, W., He, D., Zhang, C., Shi, Q.: Molecular composition and
555 spatial distribution of dissolved organic matter (DOM) in the Pearl River
556 Estuary, China, *Environ. Chem.*, 17, 2019.
- 557 He, C., Zhang, Y., Li, Y., Zhuo, X., Li, Y., Zhang, C., Shi, Q.: In-House Standard
558 Method for Molecular Characterization of Dissolved Organic Matter by FT-ICR
559 Mass Spectrometry, *ACS Omega*, 5(20): 11730-11736, 2020.
- 560 Hodas, N., Sullivan, A. P., Skog, K., Keutsch, F. N., Collett Jr, J. L., Decesari, S.,
561 Facchini, M. C., Carlton, A. G., Laaksonen, A., Turpin, B. J.: Aerosol liquid
562 water driven by anthropogenic nitrate: Implications for lifetimes of water-
563 soluble organic gases and potential for secondary organic aerosol formation,
564 *Environ. Sci. Technol.*, 48(19): 11127-11136, 2014.
- 565 Koch, B. P., Dittmar, T.: From mass to structure: an aromaticity index for high-
566 resolution mass data of natural organic matter, *Rapid Commun. Mass Spectrom.*,
567 20(5): 926-932, 2006.
- 568 Kroll, J. H., Donahue, N. M., Jimenez, J. L., Kessler, S. H., Canagaratna, M. R., Wilson,
569 K. R., Altieri, K. E., Mazzoleni, L. R., Wozniak, A. S., Bluhm, H., Mysak, E. R.,
570 Smith, J. D., Kolb, C. E., Worsnop, D. R.: Carbon oxidation state as a metric for
571 describing the chemistry of atmospheric organic aerosol, *Nat. Chem.*, 3(2): 133-
572 139, 2011.
- 573 Künzli, N., Kaiser, R., Medina, S., Studnicka, M., Chanel, O., Filliger, P., Herry, M.,
574 Horak, F., Jr., Puybonnieux-Textier, V., Quénel, P., Schneider, J., Seethaler, R.,
575 Vergnaud, J. C., Sommer, H.: Public-health impact of outdoor and traffic-related



- 576 air pollution: a European assessment, *Lancet*, 356(9232): 795-801, 2000.
- 577 Lee, B. H., Mohr, C., Lopez-Hilfiker, F. D., Lutz, A., Hallquist, M., Lee, L., Romer, P.,
578 Cohen, R. C., Iyer, S., Kurtén, T., Hu, W., Day, D. A., Campuzano-Jost, P.,
579 Jimenez, J. L., Xu, L., Ng, N. L., Guo, H., Weber, R. J., Wild, R. J., Brown, S.
580 S., Koss, A., Gouw, J. d., Olson, K., Goldstein, A. H., Seco, R., Kim, S., McAvey,
581 K., Shepson, P. B., Starn, T., Baumann, K., Edgerton, E. S., Liu, J., Shilling, J.
582 E., Miller, D. O., Brune, W., Schobesberger, S., D'Ambro, E. L., Thornton, J. A.:
583 Highly functionalized organic nitrates in the southeast United States:
584 Contribution to secondary organic aerosol and reactive nitrogen budgets, *P. Natl.*
585 *Acad. Sci. U. S. A.*, 113(6): 1516-1521, 2016.
- 586 Li, X., Song, S., Zhou, W., Hao, J., Worsnop, D., Jiang, J.: Interactions between aerosol
587 organic components and liquid water content during haze episodes in Beijing,
588 *Atmos. Chem. Phys.*, 19: 12163-12174, 2019.
- 589 Li, Y., Zhao, J., Wang, Y., Seinfeld, J. H., Zhang, R.: Multigeneration Production of
590 Secondary Organic Aerosol from Toluene Photooxidation, *Environ. Sci.*
591 *Technol.*, 55(13): 8592-8603, 2021.
- 592 Lin, P., Liu, J., Shilling, J. E., Kathmann, S. M., Laskin, J., Laskin, A.: Molecular
593 characterization of brown carbon (BrC) chromophores in secondary organic
594 aerosol generated from photo-oxidation of toluene, *Phys. Chem. Chem. Phys.*,
595 17(36): 23312-23325, 2015.
- 596 Lv, S., Wang, F., Wu, C., Chen, Y., Liu, S., Zhang, S., Li, D., Du, W., Zhang, F., Wang,
597 H., Huang, C., Fu, Q., Duan, Y., Wang, G.: Gas-to-Aerosol Phase Partitioning



- 598 of Atmospheric Water-Soluble Organic Compounds at a Rural Site in China: An
599 Enhancing Effect of NH₃ on SOA Formation, *Environ. Sci. Technol.*, 56(7):
600 3915-3924, 2022.
- 601 Mozurkewich, M.: The dissociation constant of ammonium nitrate and its dependence
602 on temperature, relative humidity and particle size, *Atmos. Environ.*, 27(2): 261-
603 270, 1993.
- 604 Müller, A., Miyazaki, Y., Tachibana, E., Kawamura, K., Hiura, T.: Evidence of a
605 reduction in cloud condensation nuclei activity of water-soluble aerosols caused
606 by biogenic emissions in a cool-temperate forest, *Sci. Rep.*, 7(1): 8452. DOI:
607 10.1038/s41598-017-08112-9., 2017.
- 608 Nguyen, T. K. V., Capps, S. L., Carlton, A. G.: Decreasing Aerosol Water Is Consistent
609 with OC Trends in the Southeast U.S, *Environ. Sci. Technol.*, 49(13): 7843-7850,
610 2015.
- 611 Nguyen, T. K. V., Zhang, Q., Jimenez, J. L., Pike, M., Carlton, A. G.: Liquid water:
612 ubiquitous contributor to aerosol mass, *Environ. Sci. Tech. Let.*, 3(7): 257-263,
613 2016.
- 614 Qiao, W., Guo, H., He, C., Shi, Q., Xiu, W., Zhao, B.: Molecular Evidence of Arsenic
615 Mobility Linked to Biodegradable Organic Matter, *Environ. Sci. Technol.*,
616 54(12): 7280-7290, 2020.
- 617 Qiu, Y., Xie, Q., Wang, J., Xu, W., Li, L., Wang, Q., Zhao, J., Chen, Y., Chen, Y., Wu,
618 Y., Du, W., Zhou, W., Lee, J., Zhao, C., Ge, X., Fu, P., Wang, Z., Worsnop, D.
619 R., Sun, Y.: Vertical Characterization and Source Apportionment of Water-



- 620 Soluble Organic Aerosol with High-resolution Aerosol Mass Spectrometry in
621 Beijing, China, ACS Earth Space Chem., 3(2): 273-284, 2019.
- 622 Sareen, N., Schwier, A., Lathem, T., Nenes, A., McNeill, V. F.: Surfactants from the gas
623 phase may promote cloud droplet formation, P. Natl. Acad. Sci. U. S. A., 110:
624 2723-2728, 2013.
- 625 Sareen, N., Waxman, E. M., Turpin, B. J., Volkamer, R., Carlton, A. G.: Potential of
626 aerosol liquid water to facilitate organic aerosol formation: assessing knowledge
627 gaps about precursors and partitioning, Environ. Sci. Technol., 51(6): 3327-
628 3335, 2017.
- 629 Schmidt, F., Koch, B. P., Goldhammer, T., Elvert, M., Witt, M., Lin, Y.-S., Wendt, J.,
630 Zabel, M., Heuer, V. B., Hinrichs, K.-U.: Unraveling signatures of
631 biogeochemical processes and the depositional setting in the molecular
632 composition of pore water DOM across different marine environments,
633 Geochim. Cosmochim. Ac., 207: 57-80, 2017.
- 634 Sihui, S., Xie, Q., Lang, Y., Cao, D., Xu, Y., Chen, J., Chen, S., Hu, W., Qi, Y., Pan, X.,
635 Sun, Y., Wang, Z., Liu, C.-Q., Jiang, G., Fu, P.: High Molecular Diversity of
636 Organic Nitrogen in Urban Snow in North China, Environ. Sci. Technol., 2021.
- 637 Simon, H., Bhave, P., Swall, J., Frank, N., Malm, W.: Determining the spatial and
638 seasonal variability in OM/OC ratios across the US using multiple regression,
639 Atmos. Chem. Phys., 11(6): 2933-2949, 2011.
- 640 Song, J., Li, M., Jiang, B., Wei, S., Fan, X., Peng, P. a.: Molecular Characterization of
641 Water-Soluble Humic like Substances in Smoke Particles Emitted from



- 642 Combustion of Biomass Materials and Coal Using Ultrahigh-Resolution
643 Electro spray Ionization Fourier Transform Ion Cyclotron Resonance Mass
644 Spectrometry, *Environ. Sci. Technol.*, 52(5): 2575-2585, 2018.
- 645 Stadnytskyi, V., Bax, C. E., Bax, A., Anfinrud, P.: The airborne lifetime of small speech
646 droplets and their potential importance in SARS-CoV-2 transmission, *P. Natl.*
647 *Acad. Sci. U. S. A.*, 117(22): 11875-11877, 2020.
- 648 Sun, Y., Du, W., Fu, P., Wang, Q., Li, J., ge, X., Zhang, q., Zhu, C., Ren, L., Xu, W.,
649 Zhao, J., Han, T., Worsnop, D., Wang, Z.: Primary and secondary aerosols in
650 Beijing in winter: Sources, variations and processes, *Atmos. Chem. Phys.*, 16:
651 8309-8329, 2016.
- 652 Tan, H., Cai, M., Fan, Q., Liu, L., Li, F., Chan, P. W., Deng, X., Wu, D.: An analysis of
653 aerosol liquid water content and related impact factors in Pearl River Delta, *Sci.*
654 *Total Environ.*, 579: 1822-1830, 2017.
- 655 Tong, H., Kourtchev, I., Pant, P., Keyte, I., O'Connor, I. P., Wenger, J., Pope, F., Harrison,
656 R., Kalberer, M.: Molecular composition of organic aerosols at urban
657 background and road tunnel sites using ultra-high resolution mass spectrometry,
658 *Faraday Discuss.*, 189: 51-68, 2016.
- 659 Wang, J., Gui, H., Yang, Z., Yu, T., Zhang, X., Liu, J.: Real-world gaseous emission
660 characteristics of natural gas heavy-duty sanitation trucks, *J. Environ. Sci.*, 115:
661 319-329, 2022.
- 662 Wang, J., Ye, J., Zhang, Q., Zhao, J., Wu, Y., Li, J., Liu, D., Li, W., Zhang, Y., Wu, C.,
663 Xie, C., Qin, Y., Lei, Y., Huang, X., Guo, J., Liu, P., Fu, P., Li, Y., Lee, H. C.,



- 664 Choi, H., Zhang, J., Liao, H., Chen, M., Sun, Y., Ge, X., Martin, S. T., Jacob, D.
665 J.: Aqueous production of secondary organic aerosol from fossil-fuel emissions
666 in winter Beijing haze, Proceedings of the National Academy of Sciences,
667 118(8): e2022179118, 2021.
- 668 Xie, Q., Sihui, S., Chen, S., Xu, Y., Cao, D., Chen, J., Ren, L., Yue, S., Zhao, W., Sun,
669 Y., Wang, Z., Tong, H., Su, H., Cheng, Y., Kawamura, K., Jiang, G., Liu, C.-Q.,
670 Fu, P.: Molecular characterization of firework-related urban aerosols using
671 Fourier transform ion cyclotron resonance mass spectrometry, Atmos. Chem.
672 Phys., 20: 6803-6820, 2020.
- 673 Xu, Y., Dong, X.-N., Xiao, H.-Y., Zhou, J.-X., Wu, D.-S.: Proteinaceous Matter and
674 Liquid Water in Fine Aerosols in Nanchang, Eastern China: Seasonal Variations,
675 Sources, and Potential Connections, J. Geophys. Res.: Atmos., 127(15):
676 e2022JD036589, 2022.
- 677 Xu, Y., Miyazaki, Y., Tachibana, E., Sato, K., Ramasamy, S., Mochizuki, T., Sadanaga,
678 Y., Nakashima, Y., Sakamoto, Y., Matsuda, K., Kajii, Y.: Aerosol Liquid Water
679 Promotes the Formation of Water-Soluble Organic Nitrogen in Submicrometer
680 Aerosols in a Suburban Forest, Environ. Sci. Technol., 54(3): 1406-1414, 2020a.
- 681 Xu, Y., Wu, D. S., Xiao, H. Y., Zhou, J. X.: Dissolved hydrolyzed amino acids in
682 precipitation in suburban Guiyang, southwestern China: Seasonal variations and
683 potential atmospheric processes, Atmos. Environ., 211: 247-255, 2019.
- 684 Xu, Y., Xiao, H., Wu, D., Long, C.: Abiotic and Biological Degradation of Atmospheric
685 Proteinaceous Matter Can Contribute Significantly to Dissolved Amino Acids



686 in Wet Deposition, *Environ. Sci. Technol.*, 54(11): 6551-6561, 2020b.

687 Yang, D., Zhu, S., Ma, Y., Zhou, L., Zheng, F., Wang, L., Jiang, J., Zheng, J.: Emissions
688 of Ammonia and Other Nitrogen-Containing Volatile Organic Compounds from
689 Motor Vehicles under Low-Speed Driving Conditions, *Environ. Sci. Technol.*,
690 56(9): 5440-5447, 2022.

691 Yeh, G. K., Ziemann, P. J.: Alkyl Nitrate Formation from the Reactions of C8–C14 n-
692 Alkanes with OH Radicals in the Presence of NO_x: Measured Yields with
693 Essential Corrections for Gas–Wall Partitioning, *J. Phys. Chem. A*, 118(37):
694 8147-8157, 2014.

695 Yttri, K. E., Aas, W., Bjerke, A., Cape, J., Cavalli, F., Ceburnis, D., Dye, C., Emblico,
696 L., Facchini, M., Forster, C.: Elemental and organic carbon in PM₁₀: a one year
697 measurement campaign within the European Monitoring and Evaluation
698 Programme EMEP, *Atmos. Chem. Phys.*, 7(22): 5711-5725, 2007.

699 Yue, H., He, C., Huang, Q., Yin, D., Bryan, B. A.: Stronger policy required to
700 substantially reduce deaths from PM_{2.5} pollution in China, *Nat. Commun.*,
701 11(1): 1462, 2020.

702



Table 1. The number of compounds in different subgroups in different samples and the number fractions of common molecules in the same subgroup in different samples.

Sample type (Date: Mar. 23–26)	Total	CHO	Common (CHO)	Common fraction (CHO)	CHON	Common (CHON)	Common fraction (CHON)
Air spray (23)	7069	1766	1104	63%	2375	1308	55%
Ground aspersion (23)	6166	1233	990	90%	1803	1225	73%
Air spray (24)	7317	1861	804	53%	2447	1209	50%
Ground aspersion (24)	6067	1098	990	90%	1501	1308	82%
Air spray (25)	8102	2037	804	39%	2685	1209	45%
Ground aspersion (25)	5966	845	804	95%	1464	1209	83%
No water spray (A) (26)	6998	1621	1315	81%	2120	1579	74%
No water spray (B) (26)	6990	1539	1315	85%	1963	1579	80%

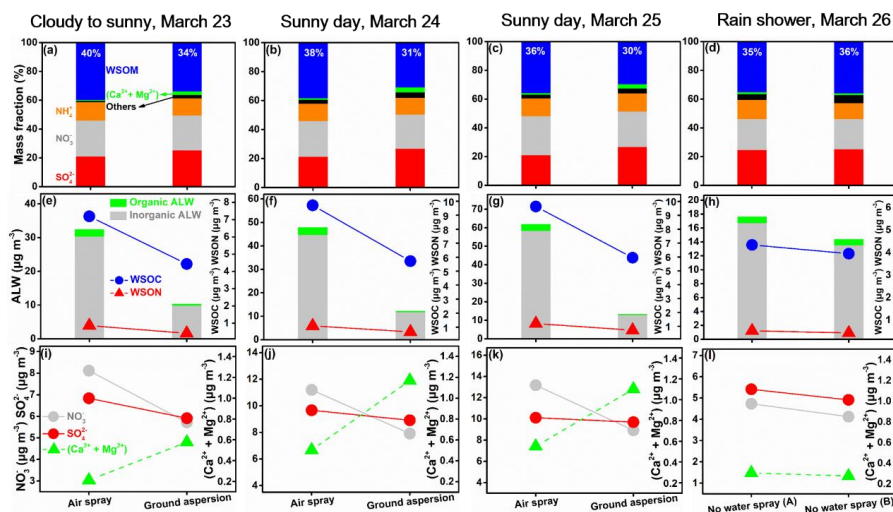


1 **Figures 1–7**

2

3

4 **Figure 1.**



5

6 **Figure 1.** The mass fractions of the chemical components in PM_{2.5}: (a, b, and c) air
 7 spray road segment vs ground aspersion road segment and (d) no water spray road
 8 segment (A) vs no water spray road segment (B). The mass concentrations of nitrate,
 9 ammonium, and the sum of calcium and magnesium in PM_{2.5}: (e, f, and g) air spray
 10 road segment vs ground aspersion road segment and (h) no water spray road segment
 11 (A) vs no water spray road segment (B). The mass concentrations of ALW, WSOC, and
 12 WSOM in PM_{2.5}: (i, j, and k) air spray road segment vs ground aspersion road segment
 13 and (l) no water spray road segment (A) vs no water spray road segment (B).

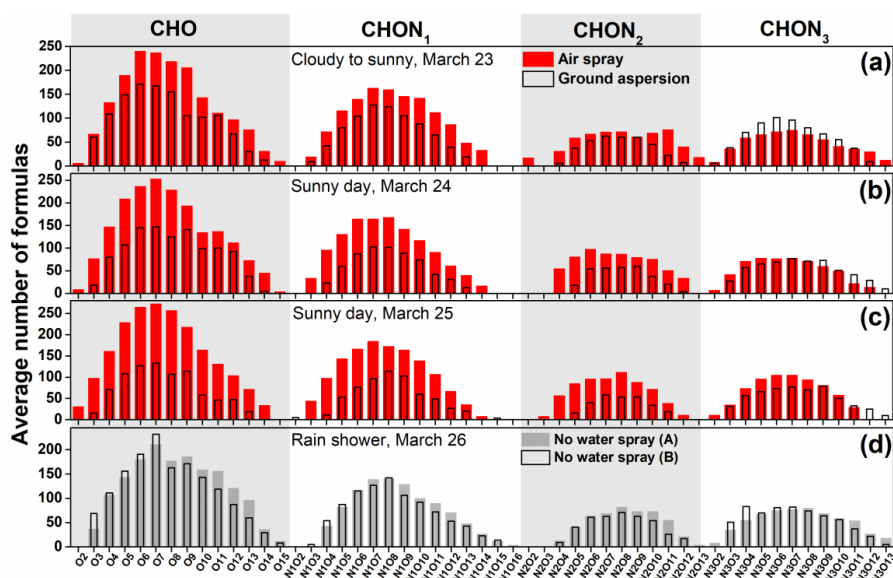
14

15



16 **Figure 2.**

17



18

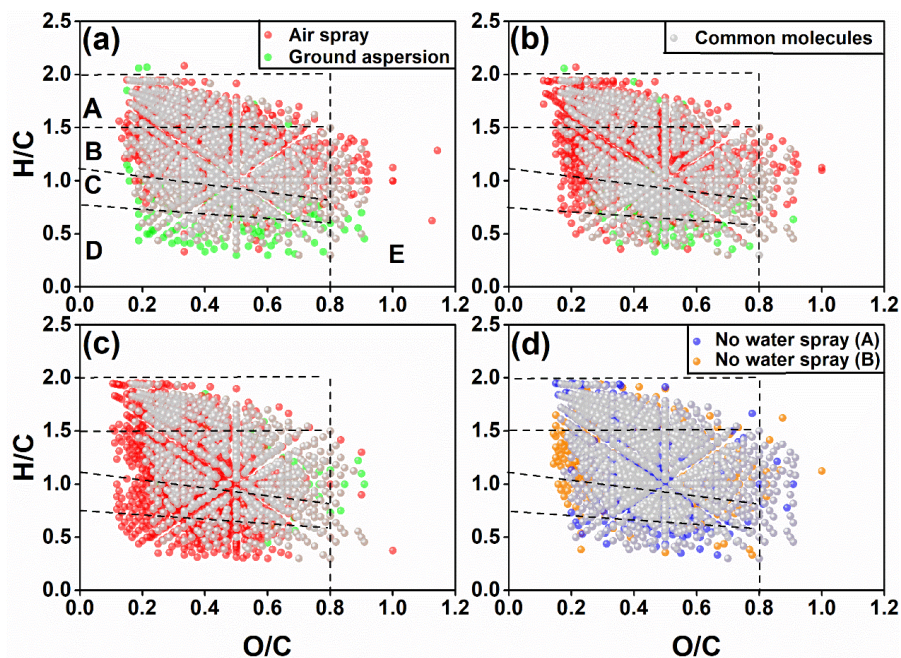
19 **Figure 2.** Classification of CHO and CHON species into subgroups according to the
20 number of O atoms in their molecules in WSOM in PM_{2.5} collected from different cases:
21 (a, b, and c) air spray road segment vs ground aspersion road segment and (d) no water
22 spray road segment (A) vs no water spray road segment (A).

23

24



25 **Figure 3**



26

27 **Figure 3.** Van Krevelen diagrams of CHO compounds in WSOM in PM_{2.5} collected
28 from different cases: air spray road segment vs ground aspersion road segment on (a)
29 March 23, (b) March 24, and (c) March 25 and two road segments without water spray
30 (A vs B) on (d) March 26. The circles of different colors indicate the unique organic
31 compounds identified in the above cases of paired comparison. Common molecules
32 identified in different cases are shown as gray circles. The classifications of compounds
33 include (A) unsaturated aliphatic-like, (B) highly unsaturated-like, (C) highly aromatic-
34 like, (D) polycyclic aromatic-like, and (E) saturated-like molecules.

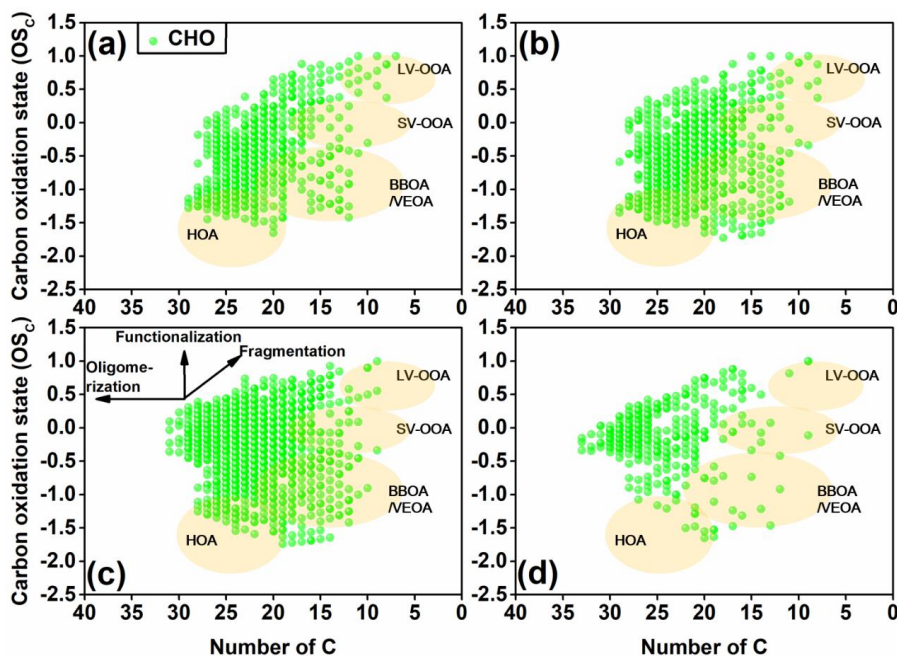
35

36



37 **Figure 4.**

38



39

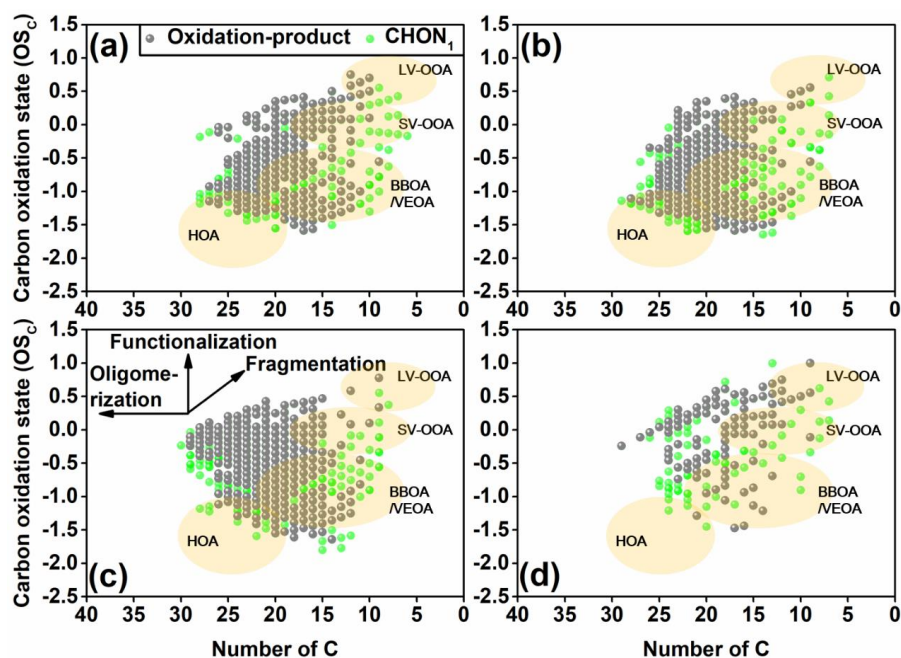
40 **Figure 4.** OS_C of unique CHO molecules in WSOM in $PM_{2.5}$ collected from different
41 cases: air spray road segment vs ground aspersion road segment on (a) March 23, (b)
42 March 24, and (c) March 25 and two road segments without water spray (A vs B) on (d)
43 March 26. For the above cases of paired comparison, the unique CHO compounds
44 indicate the CHO molecules identified in $PM_{2.5}$ collected from the air spray (/no water
45 spray-A) road segments. The light orange background represents areas of HOA
46 (hydrocarbon-like organic aerosol), BBOA and VEOA (biomass burning and vehicle
47 emission organic aerosols) (Kroll et al., 2011; Tong et al., 2016), SV-OOA (semivolatile
48 oxidized organic aerosols), and LV-OOA (low-volatility oxidized organic aerosols) (Kroll
49 et al., 2011).

50



51 **Figure 5.**

52



53

54 **Figure 5.** OS_C of unique $CHON_1$ molecules in WSOM in $PM_{2.5}$ collected from different
55 cases: air spray road segment vs ground aspersion road segment on (a) March 23, (b)
56 March 24, and (c) March 25 and two road segments without water spray (A vs B) on (d)
57 March 26. For the above cases of paired comparison, the unique $CHON_1$ compounds
58 indicate the $CHON_1$ molecules identified in $PM_{2.5}$ collected from the air spray (/no
59 water spray-A) road segments. The light orange background represents areas of HOA,
60 BBOA and VEOA, SV-OOA, and LV-OOA. The grey circles refer to the identified
61 oxidation-product pairs.

62

63

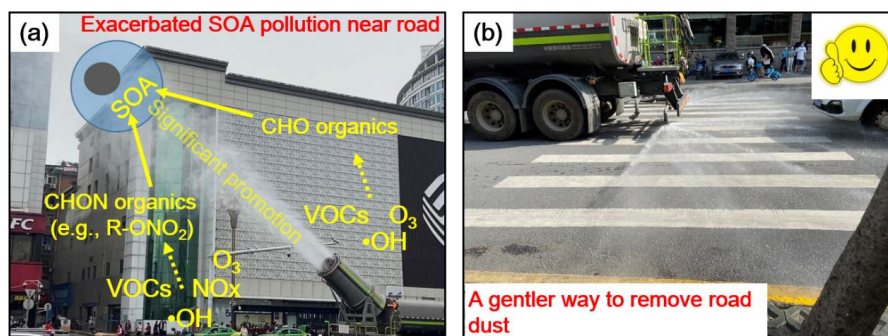
64

65



66 **Figure 6.**

67



68

69 **Figure 6.** Conceptual picture showing the influence of (a) mist cannon truck and (b)

70 traditional sprinkling truck on SOA formation in the urban road environment.

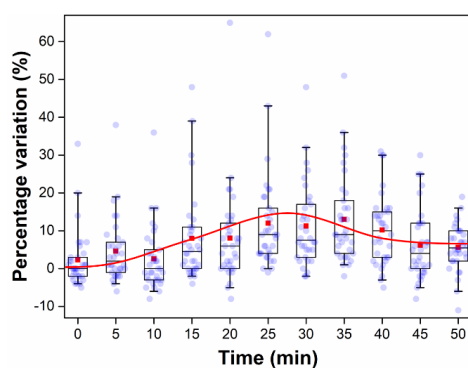
71

72



73 **Figure 7.**

74



75

76 **Figure 7.** The time series of percentage variations in $\text{PM}_{2.5}$ mass concentrations after
77 mist cannon truck operation. Each box encompasses the 25th–75th percentiles.
78 Whiskers are the 5th and 95th percentiles. The solid lines and squares inside boxes
79 indicate the median and mean. All individual data are also presented as circles.

80